

Micro Solution-Structure in O₂-H₂O Mixtures near the Critical Point Studied by Raman Spectroscopic Method

Kazuko Sugimoto¹, Mitsuo Koshi² and Seiichiro Koda^{1*}

¹Department of Chemistry, Faculty of Science and Technology, Sophia University, Kioi-cho 7-1, Chiyoda-ku, Tokyo 102-8554, Japan

²Department of Chemical System Engineering, School of Engineering, the University of Tokyo, Hongo 7-3-1, Bunkyo-ku, Tokyo 113-8656, Japan

*E-mail: s-koda@sophia.ac.jp

Density evolutions of the vibrational Raman spectra of H₂O in O₂-H₂O supercritical mixtures (O₂ mole fraction, $x_{O_2}=0.1$) and in pure H₂O were measured under the isothermal conditions (390 °C). The adopted pressure ranged from 0.2 to 39.2 MPa, including the vicinity of the critical density. In all measurements, the peak positions of the OH stretching mode of H₂O red-shifted almost linearly with fluid density up to 39.2 MPa ($\rho_r < 1.8$ at 390 °C). The band widths monotonically broadened with density. Up to the pressure of 5 MPa, the experimental band shape could be reproduced by the gas phase Raman band shape calculation. Non-symmetric feature in the band shape was attributed to the rotational structure of isolated H₂O molecules. Over 10 MPa, the spectrum could not be interpreted any more by the gas phase theory. This indicates that the spectral shape and peak position shifts were determined by the widely distributed OH stretching motions due to the H₂O - H₂O interactions. The band shapes and peak position shifts in pure H₂O and in O₂-H₂O mixtures showed almost the same dependence on the partial density of H₂O. This finding implies that the micro solution-structure of H₂O molecules are not affected significantly by the co-present O₂ molecules in the vicinity of the critical point.

1. Introduction

Supercritical water (SCW) has been attracting attention of scientists and chemical engineers working on the solution chemistry because SCW could be a new reaction or separation medium because of its specific physical properties. Many studies have been carried out on the structure of supercritical fluid (SCF) including SCW [1-14] and the reaction kinetics in SCF [15-17], intending to elucidate the potential of SCF as an alternative solvent to conventional organic solvents.

Debenedetti et al. studied the solvation structure of solute in SCF at the infinite dilution [1]. They proposed three types of solvation structure, i.e. attractive, weakly attractive, and repulsive structure, according to the excess molar volume and the Kirkwood's G factor of solute. Attractive type structures have been intensively studied with spectroscopic or simulation methods [1-3]. The review by Tucker [2] and references therein showed that the local density augmentation around a solute molecule took maximum not at the critical density

but in the lower density region. In addition, she mentioned that this type of density dependence was quite common in the attractive type supercritical mixture though she did not discuss the case of supercritical water. This density dependence is interpreted as that the solvents gather around solutes due to the solute-solvent attractive interaction under the density lower than the critical density. Here, not the density fluctuation of solvents but solute-solvent interaction plays an important role. But if the density fluctuation is larger, the situation may change. Recently Oka et al. measured the density evolution of the UV-visible spectrum of 4-nitroaniline in SCW [3]. They observed the local density augmentation maximized below but near the critical density. The difference between SCW and other supercritical fluids may be attributed to the difference of the strength of solvent-solvent interaction.

Repulsive type structures have also been studied by simulations [4-11] and experiments [12-14]. Several simulation studies have been carried out on rare gas mixtures [4], rare gases in SCW [5-7],

hydrocarbons in SCW [8, 9] and O₂ in SCW [10,11]. Some works showed that the local solvent density around solute was depressed in the vicinity of critical density. Experimental works have been carried out on rare gas mixtures [12] and also on hydrocarbons in SCW [13]. We have also investigated the density dependence of hydration structure of O₂ in SCW [14] and found that the local water density around O₂ was smaller than the bulk density in the vicinity of the critical density as predicted by the simulation study [11]. From this density dependence, we could imagine that the fluid structure of the repulsive type mixture is dominated by the density fluctuation of solvent and that the solute is merely dispersed in the low solvent density region, not strongly changing the structure.

The objective of the present work is to clarify whether O₂ molecule changes the fluctuating structure of water or not. We study the density evolutions of the Raman spectra of OH stretching motion of H₂O both in O₂-H₂O supercritical mixtures and in pure H₂O under the isothermal conditions. At first, the shapes of the OH stretching bands at several density regions are analyzed to examine what can be derived from Raman OH band analysis. Next, we compare the OH stretching bands in O₂-H₂O supercritical mixture and in pure SCW as a function of density to elucidate whether the water fluid structure is affected by the existence of O₂.

2. Experimental Methods

2.1. Experimental apparatus The experimental set-up was already described in the previous report [14]. Briefly, the experimental apparatus consisted of a Raman cell and flow systems. The cell was equipped with four sapphire windows for the spectroscopic measurements and the inlet and outlet tubings. The effective inner volume of the cell was 0.68 cm³. The body of the cell was made of Hasteloy C-276 to avoid the corrosion. Water or the aqueous H₂O₂ (Wako co. ltd.) was first pressurized with a syringe pump (ISCO, 260D) and fed to the preheating section heated up to 450 - 500°C. In this section, H₂O₂ was completely decomposed into O₂ and H₂O. Then the water or O₂-H₂O mixture was introduced into the cell heated up to the desired temperature. The effluent from the cell was cooled down through a heat exchanger with water and the pressure was reduced to the ambient pressure with a back-pressure regulator (JASCO, 880-81). The temperature of the fluid in the cell was measured by thermocouples covered with a SUS 316 sheath,

being inserted into the cell to touch the fluid directly.

Raman spectra were measured with a conventional Raman spectrometer (JASCO, NRS-2000). An Ar⁺ ion laser at 488 nm with the power of 0.4 W at the front of the cell was used as the light source. The laser light transmitted through an optical fiber was focused into the cell with a $f=50$ mm focusing lens. The backscattered light was led inversely through the optical fiber to the Raman spectrometer. The Raman signal was detected using a liquid N₂ cooled CCD detector. During the experiments, the mechanical slit width of the spectrometer was fixed at 10 μ m and the resolution of apparatus was ca. 3 cm⁻¹ at ca. 3400 cm⁻¹. The adopted temperatures were 380, 390, 400, and 500 °C for pure H₂O and 390 °C for O₂-H₂O supercritical mixtures (the O₂ mole fraction, $x_{O_2} = 0.1$). The pressure ranged from 0.2 to 39.2 MPa, covering the vicinity of the critical density.

2.2. Density of mixtures Densities of O₂-H₂O mixtures were estimated using Heiling's empirical equation as described in previous reports [14, 18]. Densities of the pure H₂O were calculated using the empirical equation [19].

3. Results and Discussion

3.1. OH stretching band shape of pure H₂O

The OH stretching bands at several different pressures are shown in Fig. 1. Especially at lower density region, the spectral shape resembles the gas phase one. The peak position is plotted against water density in Fig. 2. It shifts almost linearly to

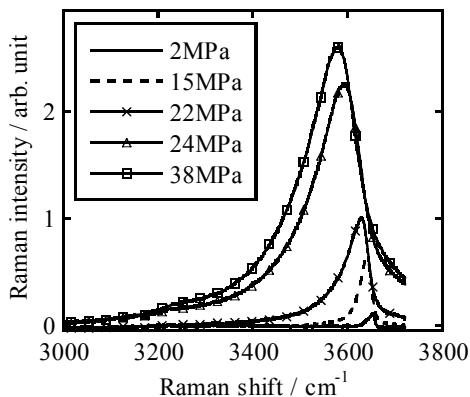


Fig. 1. The density evolution of the Raman band shape of water at 380 °C, 2-38 MPa. Densities are 0.0004, 0.0010, 0.0038, 0.0084, 0.015, 0.032 mol cm⁻³, respectively.

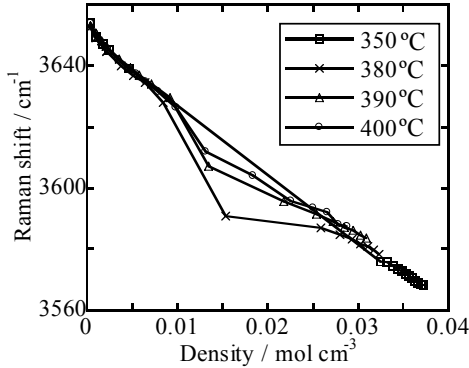


Fig. 2. The density dependence of the Raman peak position of water at 380 °C, 0.2-39.2 MPa.

the water density and the band width increases with the density. But the peak positions deviate from the line connecting the point at the density of 0 to the point at 0.04 mol cm⁻³ especially near the critical density as Kubo et al. reported [20]. The deviation from the linearity near the critical point will be discussed in later sections. In order to clarify what determines the shape and the peak position of OH stretching band under the supercritical conditions, the shapes of OH stretching bands at several density regions are first analyzed, comparing with previous Raman band shape analysis of liquid water [21–22], water vapor [23–27] and supercritical water [20, 28–30].

Raman band shape of water vapor under low-density conditions can be calculated using the rotational line positions, intensity datas and line broadening coefficients of individual rotational peaks. But under denser conditions, the rotational lines overlap each other and line-mixing will occur. Under such conditions, band shape is represented by the G-matrix formulation [31]. Both of Grisch et al. [24] and Porter et al. [25] succeeded to reproduce the Raman band shape of OH symmetric stretching mode at 293 K, 10.5 × 10⁵ Pa and 898 K, 2.0 atm, respectively. Under higher density conditions, within our knowledge, no simulation has been reported so far.

Because we measured the supercritical water from a gas density to near the critical density, our spectra should change from a gas-like to liquid like shape. At first, we calculate the Raman band shape according to the band shape theory using G-matrix as previous literatures [24, 25]. The Raman peak positions, the corresponding rotational energies of the initial states and intensities of 3000-4000 cm⁻¹

are taken from literature [27]. As the rotational relaxation matrix element of $J'\tau' \rightarrow J\tau$ inelastic transition, $W_{J\tau, J'\tau'}$, an empirical equation named quantum differentiated energy gap law (QDEGL) is employed [24–25, 32]. The equation is shown below.

For the case of $J \neq J'$ $W_{J\tau, J'\tau'}$ is

$$W_{J\tau, J'\tau''} = A(T)(2J+1)\rho_{J\tau} \exp\left(-\beta \frac{|\Delta E_{J\tau, J'\tau''}|}{kT}\right) \quad (1)$$

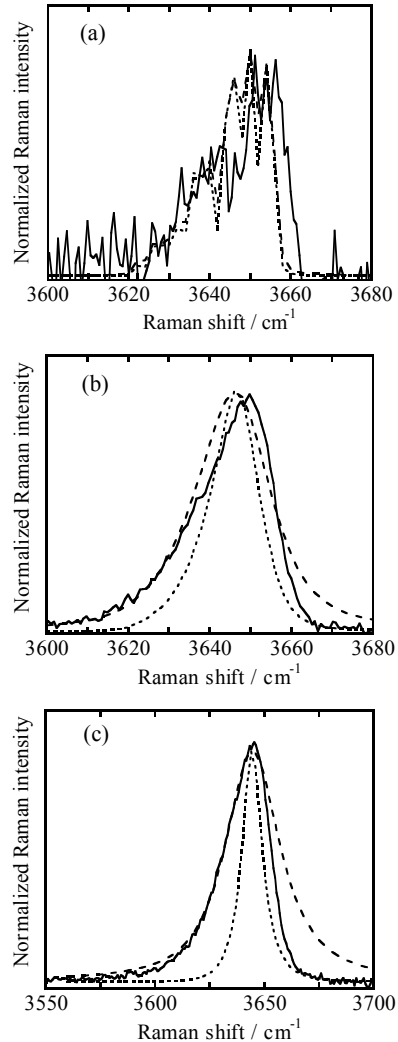


Fig. 3. The calculated and experimental Raman band shapes of water. Solid line is experimental one. Broken and dotted lines are calculated ones with and without vibrational dephasing. 380 °C, (a) 0.3 MPa, 5 × 10⁻⁵ mol cm⁻³; (b) 5 MPa, 0.0010 mol cm⁻³; (c) 10 MPa, 0.0022 mol cm⁻³.

and for $J = J'$

$$W_{J\tau, J'\tau'} = -\sum_{J \neq J'} W_{J\tau, J'\tau'} + \gamma \quad (2)$$

Here, J , Ka , and Kc are the quantum numbers of H₂O rotational state, $\tau = Ka - Kc$, and $\Delta E_{J\tau, J'\tau'}$ is the difference of the initial and final rotational energies. $\rho_{J\tau}$ is the thermal distribution of rotational state of H₂O. $A(T)$ at temperature of T K is given below.

$$A(T) = A_0 \left(\frac{T_0}{T} \right)^N \quad (3)$$

Fitting parameters are taken from Grisch et al.'s work [24]. For H₂O-H₂O collision, T_0 is 300 K, A_0 , 0.100 cm⁻¹ atm⁻¹, N , 0.78, and β , 0.21. γ is the vibrational dephasing rate. Because we didn't have any information about the vibrational dephasing rate in SCW, we took γ to be 0.0 or $0.2 \times 300 / T$ cm⁻¹ atm⁻¹ as Porter et al. [25].

The calculated spectra are shown in Fig. 3 with the corresponding experimental spectra. Below 5 MPa, the calculated and experimental spectra fairly agree. Here, non-symmetric feature in the band shape is due to the rotational structure of isolated H₂O molecules.

However over 10 MPa ($= 0.0022$ mol cm⁻³), the calculated spectra can not reproduce the experimental band shape. Calculated spectrum shows a strong collisional narrowing effect, which makes the band shape to be a Lorentzian. But the observed band shape is non-symmetric. This non-symmetric feature can not be explained by the rotational structure. It is plausible that the broad distribution of the vibrational frequency makes the spectra to be non-symmetric. The observed spectra resemble the Raman band shape of HDO in ambient water [22], where the non-symmetric feature was attributed to the non-symmetric distribution of the vibrational density of state.

Thus, over 0.0022 mol cm⁻³, Raman band shape of H₂O and its peak position may be dominated by the water solution structure. We consider that Raman band shape and its peak position could be an index of water structure or some interaction, and we can use them in the analysis of O₂-H₂O mixture structure.

3.2. The peak position of pure water

In Fig. 2, the Raman peak position shifts almost linearly. However in the vicinity of critical density the positions deviate from linearity. This density

dependence is remarkable at 380 °C, which is the closest temperature to the critical point. Such trends were also reported by Maddox et al. by MD simulation [33], Nakayama et al. for CO₂ [34], and Kubo et al. for H₂O [20].

Maddox et al. calculated the local density augmentation of ideal hypothetical supercritical fluid as a function of fluid density [33]. They observed that the local density augmentation took the maximum below the critical density.

Nakayama et al. observed the Raman spectra of CO₂ in pure supercritical CO₂ at several densities and temperatures including the critical point [34]. In their graphs of Raman peak position against the fluid density, the peak positions deviated from linearity mostly at the critical temperature. This implies that the density fluctuation determines the Raman peak position.

Although the physical meaning of the H₂O peak position is ambiguous, we consider it as an index of the extent of hydrogen bonding. In addition, under higher temperature conditions, the peak position shifts almost linearly. This implies that the peak position is linear if the density fluctuation is not present. It is plausible that the peak position reflects density fluctuation of water. To check this idea, the deviation of peak positions was plotted with the density fluctuation of water. The deviation was measured from the line obtained by the least square fitting of 350°C peak positions, which seemed not be affected by the density fluctuation. On the other hand, density fluctuation was estimated using the isothermal compressibility and density taken from literature [19]. The results are shown in Fig. 4. The temperature dependence of the intensity of peak deviation is similar to those of density fluctuation. This result supports our consideration.

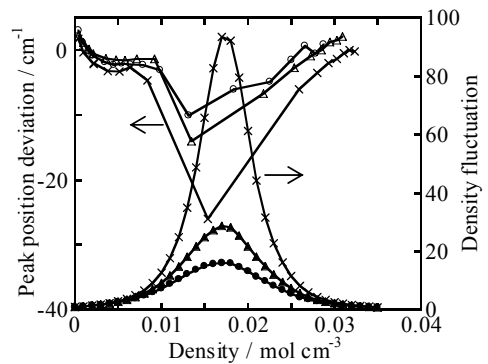


Fig.4. Deviation of the peak position from linearity and the calculated density fluctuation at three different temperatures (380, 390, 400 °C).

It is noticed, however, that the peak position deviation of H₂O is much larger than that of CO₂ if we compare CO₂ [34] and water with each other. The large deviation in H₂O can not be attributed to the simple density fluctuation alone because the density fluctuation of CO₂ at critical temperature is not so smaller than that of H₂O at 380 °C ($T_r = 1.01$). The very large deviation in water is considered to be related to the cause of the peak shift. Namely, as the density increases, the Raman band becomes wide due to the extension of hydrogen bonding. When the density fluctuation, and as a results, the

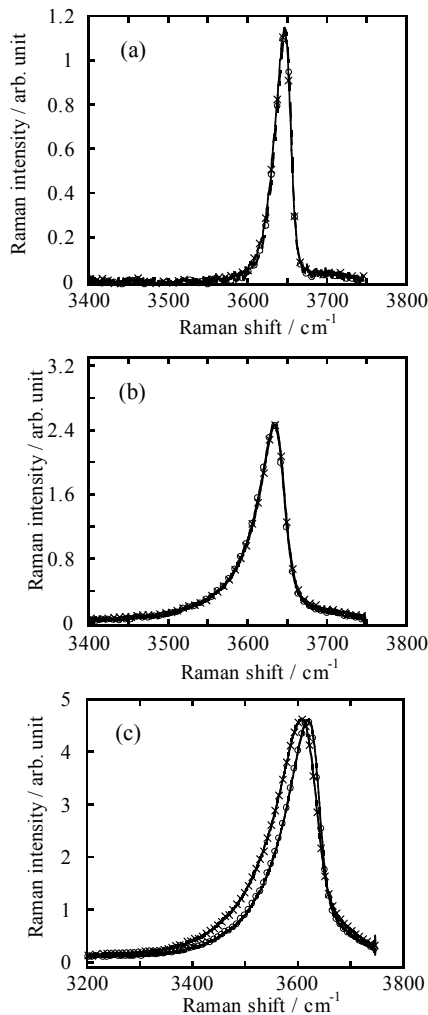


Fig. 5. OH Raman band shape in pure water and O₂(10 mol%)-H₂O mixture. Temperature is 390 °C, and densities are (a) pure H₂O (×), 0.0021; O₂-H₂O (○), 0.0020; (b) pure H₂O, 0.0092; O₂-H₂O, 0.0094; (c) pure H₂O, 0.0013; O₂-H₂O, 0.0013 mol cm⁻³.

local density augmentation around H₂O molecule occurs, the extent of hydrogen bonding may become stronger than in the homogeneous structure. This could be the cause of the large peak shift deviation.

3.3. The Comparison of band shapes and line positions in O₂-H₂O and pure H₂O Raman band shapes of OH stretching mode in pure water and a O₂-H₂O mixture possessing the same partial density of water are shown in Fig. 5. The band shapes agree very well at 0.002 and 0.009 mol cm⁻³. In the case of Fig. 5(c) the discrepancy exists because the partial densities of water in pure H₂O and the O₂-H₂O mixture are not the same.

The peak positions are plotted in Fig 6. Fig. 6(a) shows the dependence on the total fluid density and Fig. 6(b), the dependence on the water density. In Fig. 6(b), the peak positions in O₂-H₂O mixtures seem to be on the same line of pure water. This indicates that water structure is not affected by the co-present O₂ molecules.

As mentioned in the Introduction, we have measured the Raman peak shift of O₂ and have found that the local water density around O₂

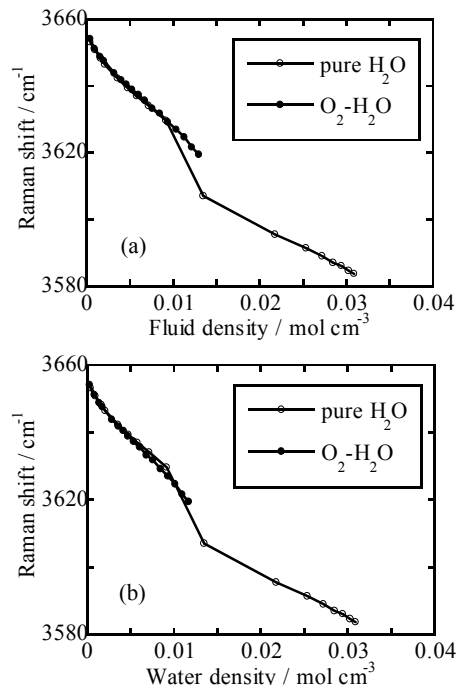


Fig. 6. OH Raman peak position of pure water and O₂(10 mol%)-H₂O mixture at 390 °C. (a): peak position against fluid density, (b): peak position against water density.

decreased mostly in the vicinity of critical density [14]. Taking account both of the above previous result and the present conclusion on the water structure, it is concluded that the fluid structure of the O₂-H₂O mixture is dominated by the density fluctuation of water and that O₂ is merely dispersed in the low water density region, which is the cause of water density depletion around O₂ in the vicinity of the critical point.

4. Conclusions

Raman band shapes of OH stretching of pure water were analyzed. Under the pressure lower than 5 MPa, the Raman band shapes could be interpreted by the collisionally broadened OH symmetric stretching mode using G-matrix formulation. However, over 10 MPa, the band shape could not be reproduced by this calculation. At these conditions, water Raman band was dominated by non-symmetric distribution of OH stretching frequency due to the fluid structure. The Raman bands measured in O₂-H₂O mixtures were compared with the bands in pure water. The results indicated that the water solution structure is not affected by the co-present O₂ molecules.

Acknowledgements

This work is supported by Research for the Future Program of the Japan Society for the Promotion of Science (96P00401), which is greatly appreciated.

References and Notes

- [1] P. G. Debenedetti, and R. S. Mohamed, *J. Chem. Phys.* **90**, 4528 (1989).
- [2] S. C. Tucker, *Chem. Rev.* **99**, 391 (1999).
- [3] H. Oka, O. Kajimoto, *Phys. Chem. Chem. Phys.* **5**, 2535 (2003).
- [4] I. B. Petsche, and P. G. Debenedetti, *J. Chem. Phys.* **91**, 7075 (1989).
- [5] A. A. Chialvo, and P. G. Debenedetti, *Ind. Eng. Chem. Res.* **31**, 1391 (1992).
- [6] P. T. Cummings, H. D. Cochran, J. M. Simonson, R. E. Mesmer, and S. Karaborni, *J. Chem. Phys.* **94**, 5606 (1991).
- [7] B. Guillot, Y. Guissani, *J. Chem. Phys.* **99**, 8075 (1993).
- [8] J. Gao, *J. Am. Chem. Soc.* **115**, 6893 (1993).
- [9] N. Matubayasi, and M. Nakahara, *J. Phys. Chem. B*, **104**, 10352 (2000).
- [10] J. M. Seminario, M. C. Concha, J. S. Murray, and P. Politzer, *Chem. Phys. Lett.* **222**, 25 (1994).
- [11] T. Ohmori, and Y. Kimura, *J. Chem. Phys.* **116**, 2680 (2002)., T. Ohmori and Y. Kimura, *J. Chem. Phys.* **119**, 7328 (2003).
- [12] A. Botti, F. Bruni, A. Isopo, G. Modesti, C. Oliva, M. A. Ricci, and R. Senesi, A. K. Soper, *J. Chem. Phys.* **118**, 235 (2003).
- [13] M. Osada, K. Toyoshima, T. Mizutani, K. Minami, M. Watanabe, T. Adschiri, and K. Arai, *J. Chem. Phys.* **118**, 4573 (2003).
- [14] K. Sugimoto, H. Fujiwara and S. Koda, *J. Supercrit. Fluid*, **32**, 293 (2004).
- [15] J. F. Brennecke, and J. E. Chateaufneuf, *Chem. Rev.* **99**, 433 (1999).
- [16] N. Akiya, and P. E. Savage, *Chem. Rev.* **102**, 2725 (2002).
- [17] S. Koda, N. Kanno, and H. Fujiwara, *Ind. Eng. Chem. Res.* **40**, 3861 (2001).
- [18] M. Christoforakos, and E. U. Franck, *Ber. Bunsenges. Phys. Chem.* **90**, 780 (1986).; M. Heiling and E. U. Franck, *Ber. Bunsenges. Phys. Chem.* **94**, 27 (1990).; M. Heiling and E. U. Franck, *Ber. Bunsenges. Phys. Chem.* **93**, 898 (1989).
- [19] W. Wagner, and A. Pruss, *J. Phys. Chem. Ref. Data* **31**, 387 (2002).
- [20] M. Kubo, N. Matubayasi, and M. Nakahara, *25th Symposium on Solution Chemistry*, Toyonaka, Osaka, Japan, (2002).
- [21] E. U. Franck, *Pure Appl. Chem.* **24**, 13 (1970).
- [22] W. Kohl, H. A. Lindner and E. U. Franck, *Ber. Bunsenges. Phys. Chem.* **95**, 1586 (1991).
- [23] C. Delaye, J. -M. Hartmann, and J. Taine, *Appl. Opt.* **28**, 5080 (1989).
- [24] F. Grisch and M. Péalat, *J. Raman Spectrosc.* **25**, 145 (1994).
- [25] F. M. Porter and D. R. Williams, *Appl. Phys. B*, **54**, 103 (1992).
- [26] B. Labani, J. Bonamy, D. Robert, and J. M. Hartmann, *J. Chem. Phys.* **87**, 2181 (1987).
- [27] G. Avila, J. M. Fernández, B. Maté, G. Tejada, and S. Montero, *J. Mol. Spectrosc.* **196**, 77 (1999).
- [28] G. E. Walfaren, M. R. Fisher, M. S. Hokmabadi, and W. -H. Yang, *J. Chem. Phys.* **85** 6970 (1986).
- [29] G. E. Walrafen, W. -H. yang, and Y. C. Chu, *J. Phys. Chem. B*, **103**, 1322 (1999).
- [30] Y. Ikushima, K. Hatakeda, N. Saito, and M. Arai, *J. Chem. Phys.* **108**, 5855 (1998).
- [31] A. I. Burshtein, and S. I. Temkin, *Spectroscopy of molecular rotation in gases and liquids* (Cambridge University Press, Cambridge, 1994).
- [32] D. A. Greenhalgh and L. A. Rahn, *J. Raman Spectrosc.* **21**, 847 (1990).
- [33] M. W. Maddox, G. Goodyear, and S. C. Tucker, *J. Phys. Chem. B* **104**, 6248 (2000).
- [34] H. Nakayama, K. Saitow, M. Sakashita, K. Ishii, and K. Nishikawa, *Chem. Phys. Lett.* **320**, 323-327 (2000).